

Introduction

A cylindrical aluminum cavity resonator was used to measure the complex permittivity of various dielectric materials by means of perturbation theory. The resonant frequencies of the empty cavity can be compared to the resonant frequencies of a cavity containing a dielectric material, to find the complex permittivity of the material. The change in the frequency can be used to find the real part of the material's complex permittivity, and the change in the quality factor (Q), of the frequency's peak, can be used to find the imaginary part. This method of complex permittivity evaluation is a use of the perturbation theory in conjunction with the complex eigenfrequency of resonance.

Theory

An electrical signal having voltage and current can be represented in terms of the wave propagation of its electric field (E) and magnetic field (H). When an electric field enters a cavity of a conducting material, the E-field must drop to zero at the walls of the cavity in accordance with Maxwell's equations. The energy carried by the wave must be conserved, forcing the cavity to store this energy in standing waves which oscillate at nodes on the boundaries of the cavity, where the electric field is zero. In an unbounded medium, the electromagnetic (EM) wave will oscillate as transverse electric and transverse magnetic (TEM), since there is no boundary to delineate which wave is not propagating transversely. In the bounded cavity, however, the standing waves will propagate such that only the E-field or H-field are transverse to the direction of propagation. This limits the waves in the cavity to two modes of propagation: transverse electric (TE), and transverse magnetic (TM). The propagation patterns for some of the lowest resonant frequencies, in these modes, are shown below.

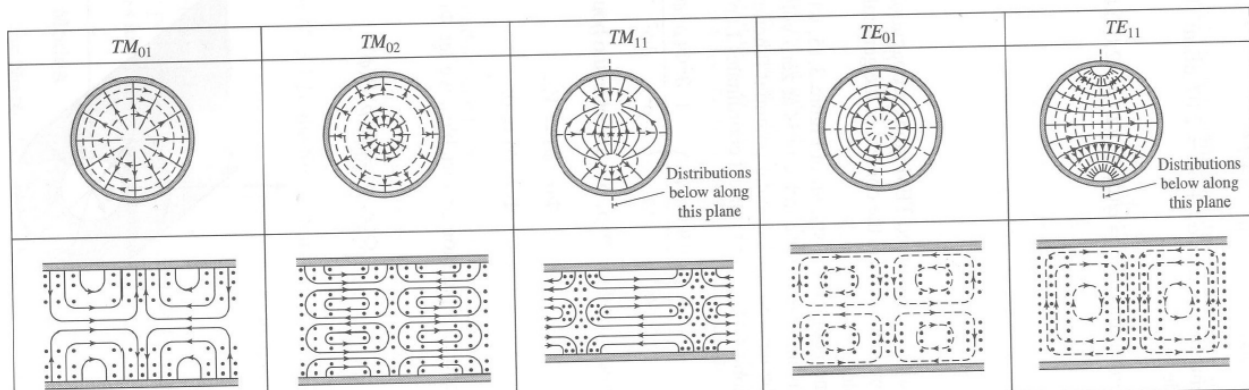


Figure 1: propagation of EM waves in a cylinder [Pozar]

In a cylindrical cavity the E-field and H-field are best realized by their cylindrical coordinate components; r , ϕ , and z . With Maxwell's equations and some algebra, all non- z components of the E-field and H-field can be expressed in terms of their z component as shown.

$$\nabla \times \bar{\mathbf{E}} = \frac{1}{r} \begin{vmatrix} \hat{r} & r\hat{\phi} & \hat{z} \\ \frac{\partial}{\partial r} & \frac{\partial}{\partial \phi} & \frac{\partial}{\partial z} \\ E_r & rE_\phi & E_z \end{vmatrix} = -j\omega\mu\bar{\mathbf{H}}$$

$$\nabla \times \bar{\mathbf{H}} = \frac{1}{r} \begin{vmatrix} \hat{r} & r\hat{\phi} & \hat{z} \\ \frac{\partial}{\partial r} & \frac{\partial}{\partial \phi} & \frac{\partial}{\partial z} \\ H_r & rH_\phi & H_z \end{vmatrix} = j\omega\epsilon\bar{\mathbf{E}}$$

$$E_r = \frac{-j}{k_c^2} \left(\beta \frac{\partial E_z}{\partial r} + \frac{\omega\mu}{r} \frac{\partial H_z}{\partial \phi} \right)$$

$$E_\phi = \frac{-j}{k_c^2} \left(\frac{\beta}{r} \frac{\partial E_z}{\partial \phi} - \omega\mu \frac{\partial H_z}{\partial r} \right)$$

$$H_r = \frac{j}{k_c^2} \left(\frac{\omega\epsilon}{r} \frac{\partial E_z}{\partial \phi} - \beta \frac{\partial H_z}{\partial r} \right)$$

$$H_\phi = \frac{-j}{k_c^2} \left(\omega\epsilon \frac{\partial E_z}{\partial r} + \frac{\beta}{r} \frac{\partial H_z}{\partial \phi} \right)$$

Figure 2: cylindrical component representation by z components [Kwok]

Evaluating E_z using Poisson's equation, and relating it to arbitrary functions of r and ϕ , it can be shown that E_z reduces to the Bessel equation.

$$E_z(r, \phi, z) = (A \sin(n\phi) + B \cos(n\phi)) J_n(k_c r) e^{j(\omega t - \beta z)}$$

Figure 3: E_z in terms of the Bessel function [Kwok]

With E_z found, all cylindrical components in Figure 2 can be solved.

Cavity perturbation theory says that the difference in the resonant complex eigenfrequency of a cavity, due to a perturbation, can be expressed by the difference in the complex permittivity of the transmission mediums, the original and the one causing the perturbation. The equation below shows the exact relationship.

$$\frac{\Delta \tilde{f}}{f_0} = - \frac{\int_{V_s} (\Delta \epsilon \mathbf{E} \cdot \mathbf{E}_0^* + \Delta \mu \mathbf{H} \cdot \mathbf{H}_0^*) d\tau}{\int_{V_c} (\epsilon \mathbf{E} \cdot \mathbf{E}_0^* + \mu \mathbf{H} \cdot \mathbf{H}_0^*) d\tau}$$

Figure 4: underlying equation of cavity perturbation theory [Meng]

The value \tilde{f} is the complex eigenfrequency, which has the frequency as its real part and the inverse of its quality factor as its imaginary part. Using a dielectric sample to perturb a dielectric propagation medium, no change will be seen in the permeability, and the term goes to zero. If a small enough region of the cavity is perturbed, then it can be assumed that E and H have similar magnitudes and the above equation can be simplified.

$$\frac{\Delta \tilde{f}}{f_0} \simeq - \frac{\int_{V_s} \Delta \epsilon \mathbf{E}_{\text{int}} \cdot \mathbf{E}_0^* d\tau}{2 \int_{V_c} \epsilon |E_0|^2 d\tau}$$

Figure 5: simplified equation of cavity perturbation theory [Meng]

If the cavity is filled with air, or a material of relative permittivity equal to one, then the complex permittivity of the perturbing material can be expanded, and the above equation can be written as shown below.

$$\begin{aligned} \frac{\Delta \tilde{f}}{f_0} &\simeq - \frac{\int_{V_s} (\epsilon' - 1 - j\epsilon'') \mathbf{E}_{\text{int}} \cdot \mathbf{E}_0^* d\tau}{2 \int_{V_c} |E_0|^2 d\tau} \\ &= - \frac{\int_{V_s} (\epsilon' - 1) \mathbf{E}_{\text{int}} \cdot \mathbf{E}_0^* d\tau}{2 \int_{V_c} |E_0|^2 d\tau} + j \frac{\int_{V_s} \epsilon'' \mathbf{E}_{\text{int}} \cdot \mathbf{E}_0^* d\tau}{2 \int_{V_c} |E_0|^2 d\tau} \end{aligned}$$

Figure 6: expansion of previous equation showing complex permittivity [Meng]

Relating the real and imaginary parts of the equation above, to the real and imaginary parts of the complex eigenfrequency, the equations below can be solved for to find the real and imaginary parts of the perturbing material's complex permittivity.

$$\epsilon' \simeq 1 - 2C_{\text{conv}} \frac{\Delta f}{f_0}$$

$$\epsilon'' \simeq C_{\text{conv}} \left(\frac{1}{Q} - \frac{1}{Q_0} \right)$$

$$C_{\text{conv}} = \frac{\int_{V_e} |E_0|^2 d\tau}{\int_{V_s} \mathbf{E}_{\text{int}} \cdot \mathbf{E}_0^* d\tau}$$

Figure 7: equations to find complex permittivity

Subscripts of zero, in all equations above, refer to the unperturbed frequencies and quality factors. Those values without subscripts refer to frequencies and quality factors due to perturbations. E_{int} refers to the E-field inside the sample perturbing the cavity.

By recording the frequency and quality factors with and without perturbing materials, the values recorded can then be used in the above set of equations to find the complex permittivity. The E-field values can be found for a cylindrical cavity, by using the identities given earlier for cylindrical components of an E-field. The direction of the E-field, giving E-field components present, can be seen by analyzing the propagation patterns in Figure 1.

Quality factors can be calculated in a number of ways. The simplest and most common is the full-width half-max method. In this method, the frequencies at -3dB to the left and right of the peak frequency are recorded and their difference taken. Dividing the peak frequency, gives the quality factor at that frequency. A ratio of the energy stored, to the energy dissipated.

A resonant cavity given two ports acts as a symmetrical two port network. This simplifies positioning of ports, when measuring frequencies.

Procedure

An aluminum cylinder with radius 0.9025" and length 2.25" was used as the resonant cavity. Mounting holes were drilled to place electrical couplers at the top and bottom, and 180° from each other on the side walls.

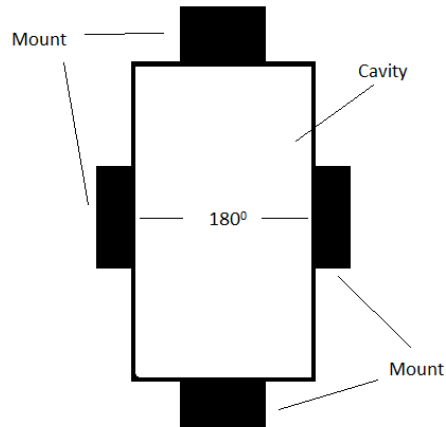


Figure 8: cavity showing position of mounting holes

The electrical couplers were placed in three configurations to read resonant frequencies below 6GHz using a network analyzer measuring S_{21} . The first configuration placed the horizontal couplers 180° apart from each other, on the side walls of the cavity, and measured TE_{111} and TM_{011} modes. Mode TM_{011} was not used to calculate complex permittivity. The second configuration placed the couplers vertically at the top and bottom of the cylinder. In this configuration TM_{010} and TM_{011} were seen. Again TM_{011} was not used. In the final configuration the couplers were placed with one coupler at the top of the cylinder and one coupler at the side. In this configuration, only the unused TM_{011} mode was seen.

In the first configuration, with couplers placed horizontally, a resonant frequency of an empty cavity for TE_{111} was recorded as the maximum value of the peak at this frequency. The network analyzer was set to center its screen at this frequency with a span of 30MHz. The reference value was set to 5dB below the peak value and the reference position was placed at one division from the bottom of the network analyzer's screen. The scale was set to 0.6dB per division. This setting was used for all measurements with the reference value changing based on the magnitude of the peak, and the center frequency changing based on its current value. The marker of the network analyzer was moved -3dB to the left and right of the peak magnitude and these frequencies were recorded to calculate the Q at this frequency, by the method described earlier.

With an initial resonant frequency and Q, dielectric samples were placed in the cavity. Three materials were tested: Kel-F, Teflon, and Delrin. Of these materials, two geometries and sizes were used. Kel-F had one sample size and geometry: a cylinder of radius 0.03" and length 0.375". The Delrin came in one geometry and two sizes: squares 0.0625" thick, one 0.5"x0.5" and the other 0.1875"x 0.1875". The Teflon came in all the sizes and geometries mentioned for the other two, plus a shorter cylinder of length 0.25". The samples had to be placed in the E-field to be calculated, and in the first configuration, TE_{111} , this required the sample to be directly in the middle of the cavity. Styrofoam was used as a shelf to hold the samples directly in the middle of the cavity, since its dielectric constant is close to that of air's.

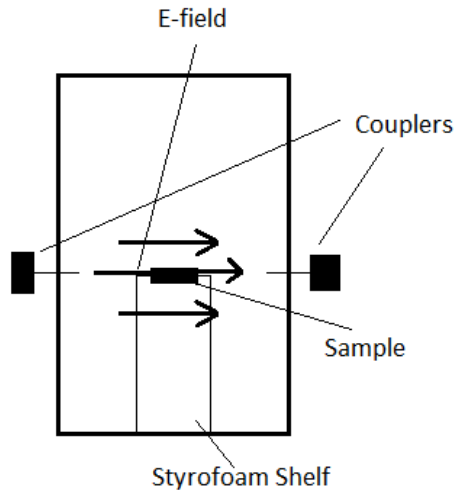


Figure 9: TE_{111} mode propagation and sample setup in cavity

The three frequencies described above were recorded for all samples in this configuration. All geometries were laid horizontal on the Styrofoam shelf.

In the second configuration the same measurements were taken, first without samples, and then with. All samples were placed vertically at the bottom of the cavity on a Styrofoam mount to keep them upright. The third configuration was not used since that mode was not calculated for.

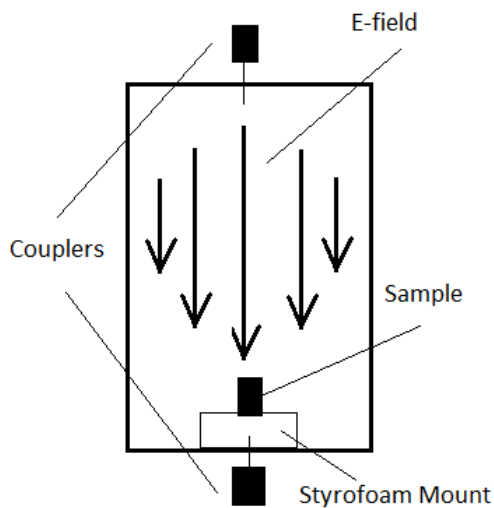


Figure 10: TM_{010} mode propagation and sample setup in cavity

Once values had been recorded for all samples in both configurations, the complex permittivities were solved for using the equations given in the above figures. The E-field in the sample was assumed to have the same magnitude as the E-field in that portion of the cavity, a reasonable assumption for samples much smaller than the cavity itself. TE_{111} mode calculations assumed that all the magnitude of

b	Ds		dc		e'	e''	loss tan	
0.03	0.375		2.25		6.70E+03	765.5858492	-1.14E-01	
f0		lowf0	highf0		1/Q0	1/Q	Cconv	
4.54E+09		4.53E+09	4.54E+09		3.63E-03	3.91E-03	2816241	
f		lowf	highf		den	num		dc/ds
4.53E+09		4.52E+09	4.54E+09		8.62E-07	0.4046		6

Table 3: Short Cylindrical Teflon in TE₁₁₁ mode

Cylindrical Sample		teflon, short						
b	Ds		dc		e'	e''	loss tan	
0.03	0.25		2.25		8.10E+03	319.5660667	-3.94E-02	
f0		lowf0	highf0		1/Q0	1/Q	Cconv	
4.54E+09		4.53E+09	4.54E+09		3.63E-03	3.71E-03	4224362	
f		lowf	highf		den	num		dc/ds
4.53E+09		4.52E+09	4.54E+09		8.62E-07	0.4046		9

Table 4: Large Rectangular Teflon in TE₁₁₁ mode

large Teflon							
x	Y	z	dc		e'	e''	loss tan
0.5	0.5	0.0625	2.25		-13.103	0.116067181	-8.86E-03
f0		lowf0	highf0		1/Q0	1/Q	Cconv
4.54E+09		4.53E+09	4.54E+09		0.003635	0.003704048	1679.032
f		lowf	highf		num	den	
4.52E+09		4.51E+09	4.53E+09		0.91035	0.000542188	

Table 5: Small Rectangular Teflon in TE₁₁₁ mode

small Teflon							

x	Y	z	dc		e'	e''	loss tan
0.1875	0.1875	0.0625	2.25		-17.952	-0.05246055	2.92E-03
f0		lowf0	highf0		1/Q0	1/Q	Cconv
4.54E+09		4.53E+09	4.54E+09		0.003635	0.003630527	11939.78
f		lowf	highf		num	den	
4.53E+09		4.52E+09	4.54E+09		0.91035	7.62451E-05	

Table 6: Large Rectangular Delrin in TE₁₁₁ mode

large delrin							
x	Y	z	dc		e'	e''	loss tan
0.5	0.5	0.0625	2.25		-19.6177	-0.1511255	7.70E-03
f0		lowf0	highf0		1/Q0	1/Q	Cconv
4.54E+09		4.53E+09	4.54E+09		0.003635	0.003544913	1679.032
f		lowf	highf		num	den	
4.51E+09		4.50E+09	4.52E+09		0.91035	0.000542188	

Table 7: Small Rectangular Delrin in TE₁₁₁ mode

small delrin							
x	Y	z	dc		e'	e''	loss tan
0.1875	0.1875	0.0625	2.25		-24.7958	0.821645158	-3.31E-02
f0		lowf0	highf0		1/Q0	1/Q	Cconv
4.54E+09		4.53E+09	4.54E+09		0.003635	0.003703736	11939.78
f		lowf	highf		num	den	
4.53E+09		4.52E+09	4.54E+09		0.91035	7.62451E-05	

Table 8: Cylindrical Kel-F in TM₀₁₀ mode

Cylindrical Sample	kel-F						
b	Ds		dc		e'	e''	loss tan

0.03	0.375		2.25		-2.91145	3.2943004	1.13E+00	
f0		lowf0	highf0		1/Q0	1/Q	Cconv	
5.03E+09		5.03E+09	5.04E+09		0.003031	3.3902E-12	1086.750221	
f		lowf	highf		den	num		dc/ds
5.03E+09		5.017381	5.034418		6.11E-04	0.1107		6

Table 9: Long Cylindrical Teflon in TM₀₁₀ mode

Cylindrical Sample		teflon, long						
b	Ds		Dc		e'	e''	loss tan	
0.03	0.375		2.25		2.07E+00	1.073031152	-5.19E-01	
f0		lowf0	highf0		1/Q0	1/Q	Cconv	
5.04E+09		5.03E+09	5.04E+09		2.53E-03	3.51E-03	1086.75	
f		lowf	highf		den	num		dc/ds
5.03E+09		5.02E+09	5.04E+09		6.11E-04	0.1107		6

Table 10: Short Cylindrical Teflon in TM₀₁₀ mode

Cylindrical Sample		teflon, short						
b	Ds		Dc		e'	e''	loss tan	
0.03	0.25		2.25		2.84E+00	1.583914636	-5.58E-01	
f0		lowf0	highf0		1/Q0	1/Q	Cconv	
5.04E+09		5.03E+09	5.04E+09		2.53E-03	3.50E-03	1630.125	
f		lowf	highf		den	num		dc/ds
5.03E+09		5.02E+09	5.04E+09		6.11E-04	0.1107		9

Table 11: Large Rectangular Teflon in TM₀₁₀ mode

large Teflon							

x	Y	Z	dc		e'	e''	loss tan
0.5	0.5	0.0625	2.25		-5.2156	0.92921097	-1.78E-01
f0		lowf0	highf0		1/Q0	1/Q	Cconv
5.04E+09		5.04E+09	5.05E+09		0.002321	0.003504352	785.2610837
f		lowf	highf		num	den	
5.02E+09		5.01E+09	5.03E+09		0.249075	0.000317188	

Table 12: Small Rectangular Teflon in TM_{010} mode

small Teflon							
x	Y	Z	dc		e'	e''	loss tan
0.1875	0.1875	0.0625	2.25		-9.63455	1.266430088	-1.31E-01
f0		lowf0	highf0		1/Q0	1/Q	Cconv
5.04E+09		5.04E+09	5.05E+09		0.002321	0.00254783	5584.078818
f		lowf	highf		num	den	
5.04E+09		5.03E+09	5.04E+09		0.249075	4.46045E-05	

Table 13: Large Rectangular Delrin in TM_{010} mode

large delrin							
X	Y	Z	dc		e'	e''	loss tan
0.5	0.5	0.0625	2.25		-8.82969	0.862689667	-9.77E-02
f0		lowf0	highf0		1/Q0	1/Q	Cconv
5.04E+09		5.04E+09	5.05E+09		0.002321	0.003419639	785.2611
F		lowf	highf		num	den	
5.01E+09		5.00E+09	5.02E+09		0.249075	0.000317188	

Table 14: Small Rectangular Delrin in TM_{010} mode

small delrin							
X	Y	Z	dc		e'	e''	loss tan

0.1875	0.1875	0.0625	2.25		-13.1794	1.490568029	-1.13E-01
f0		lowf0	highf0		1/Q0	1/Q	Cconv
5.04E+09		5.04E+09	5.05E+09		0.002321	0.002587969	5584.079
F		lowf	highf		num	den	
5.03E+09		5.03E+09	5.04E+09		0.249075	4.46045E-05	

Discussion

Values found online for the complex permittivity of each of these materials are given in the table below.

Material	ϵ'	ϵ''
Kel-F	2.6	0.0364
Teflon	2.1	0.00059
Delrin	3.7	0.0185

None of the calculated values are close to the expected values. The best results come from cylindrical samples in TM_{010} mode. TM_{010} mode has been shown to give accurate values when used in the same manner as done in this experiment. This mode is the easiest to calculate for and is unlikely that calculation errors were made. Measuring the quality factor was the most difficult, as it seems this value needs to be very precise for accurate results. The setup of the network analyzer for this measurement was close to the limits of the network analyzer's resolution for the requirements of this project, and cannot be made better without a new machine. This makes accurate Q measurements unlikely. It is likely that assumptions made for calculations involving square samples, were too egregious. Samples are also likely to have been too large. It was found that the size of the sample is important. Permittivity values for the small and large cylindrical samples in TM_{010} mode vary quite a bit. It is believed the size needs to be large enough to make a perturbation easy to measure, but not so large as to drastically effect assumptions made in calculation. Finding the perfect sized samples may be a difficult task. It is also likely that calculation errors were made in evaluating TE_{111} modes. This mode was assumed to propagate entirely in the radial direction, but the field lines show azimuthal theta components since they do not isotropically radiate from the center. Values for cylindrical samples in this mode give credit to this likelihood. In general, all values showed increases and decreases for expected materials, even where the values are multiple orders of magnitude away from the expected value.

Conclusion

Future experiments will be conducted to narrow in on the source of the problems. The measurement procedure will need to be refined in the future. Assumptions made for the TE_{111} will be clarified so that

this mode can be used. TE_{111} mode is important, since it is the most fundamental mode, at the lowest allowed frequency. Dielectric resonators and antenna reflections will also be explored, and results for these experiments will be compared to those found in this paper, and the hopefully better results for cavity perturbation found in later papers.

References

Kwok, Ray. *Waveguides*. EE172 lecture slides. San Jose State University. Pdf.
www.engr.sjsu.edu/rkwok/

Kwok, Ray. *Cavity Resonator*. EE172 lecture slides. San Jose State University. Pdf.
www.engr.sjsu.edu/rkwok/

Pozar, David M. *Microwave Engineering*. Third Edition. Wiley. 2005

Meng, Binshen, Booske, John, Cooper, Reid. *Extended Cavity Perturbation Technique to Determine the Complex Permittivity of Dielectric Materials*. IEEE Transactions on Microwave Theory and Techniques, Vol. 43, No. 11, Nov. 1995

Web Sources

RF Café

<http://www.rfcafe.com/references/electrical/dielectric-constants-strengths.htm>

Wikipedia

http://en.wikipedia.org/wiki/Cavity_Perturbation_Theory